

Inhibition Effect of *Coleus forskohlii* leaf extract on Steel Corrosion in 1.0 M HCl Solution: Experimental and Theoretical Approaches

Ismat H. Ali^{1*}, Riadh Marzouki^{1,2}, Youssef Ben Smida³, Ameni Brahmia⁴, Mohamed Faouzi Zid²

¹ Department of Chemistry, College of Science, King Khalid University, Abha 61413, Saudi Arabia.

² Université de Tunis El Manar, Laboratoire de Matériaux, Cristallographie et Thermodynamique Appliquée, Faculté des Sciences de Tunis, El Manar II, 2092 Tunis, Tunisia.

³ National Center of Materials Sciences Research, Technopole Borj Cedria, BP 73, 8027 Soliman, Tunisia.

⁴ Materials Chemistry and the Environment Research Unit, University of Tunis El Manar, 2092 Tunis, Tunisia.

*E-mail: ismathassanali@gmail.com

Received: 10 August 2018 / Accepted: 17 September 2018 / Published: 5 November 2018

The inhibitive performance of *Coleus forskohlii* leaf extract on mild steel corrosion process in 1.0 M HCl aqueous solutions was studied. Several methods have been adopted such as, mass loss, Tafel polarization curves as well as electrochemical impedance spectroscopy (EIS). The inhibition effectiveness was found to increase as the inhibitor concentration increased. The impact of temperature on corrosion inhibition was studied by using EIS method. The thermodynamic parameters (activation energy, free energy change and entropy change) were calculated. The inhibitor under study is classified as a mixed type inhibitor. Adsorption isotherms models were examined. Adsorption process obeys Langmuir model. The electronic properties concluded from DFT calculations were exploited to give more understandings to the action approach of studied inhibitor. Scanning electron microscope (SEM) and Energy-dispersive X-ray spectroscopy (EDS) were used to explore the efficiency of the inhibitor. The obtained results confirmed the effectiveness of the studied inhibitor.

Keywords: mild steel; acid solution; *Coleus forskohlii* ; inhibition ; corrosion; DFT

1. INTRODUCTION

Corrosion is a severe phenomenon that affects alloys and metals and diminishes the value and efficiency of metallic and alloyed products and shortens their life time. Corrosion is a global problem,

for example, a study in United States of America showed that the total annual corrosion cost is around 276 billion \$ which represents 3.1% of the gross budget. The corrosion cost in water sector is reported to be about 36 billion \$. The study showed that, though the management of corrosion has been improved during the few previous years but the United States must make greater efforts in the field of scientific research to combat corrosion [1].

Usually treatment of corrosion is performed by addition of synthesized organic chemicals to the medium where metals and alloys are present. Corrosion prevention is attainable more than complete removal. The excellent technique of protecting steel and other alloys against deterioration due to corrosion process is by the usage of inhibitors. Synthetic organic compounds having heteroatoms, π electrons and electronegative functional groups or conjugated double bonds are normally adopted to minimize the corrosion attack on metals in acidic media [2-12]. Generally, the surface of a metal is covered by those adsorbed compounds. Hence, they block active corrosion positions. However, the major problems related to most of chemical inhibitors are, their high cost and negative effect on the environment because of their toxicity.

Recently, natural products have attracted some attention as green corrosion inhibitors [13-22]. These constituents can be obtained using simple procedure with low cost. Most of these products are nontoxic and biodegradable in nature.

The positive results achieved from natural constituents have motivated us to test the use of *Coleus forskohlii* leaf extract (CFLE). In this work, CFLE was evaluated as eco-friendly corrosion inhibitor for acidic environment. Mass loss tests and electrochemical measurements were employed to examine the efficiency of CFLE in 1.0 M HCl aqueous solutions.

2. EXPERIMENTAL

2.1. Collection and preparation of plant

The leaves of *Coleus forskohlii* were collected randomly from Alsoda, Asir area, south of Saudi Arabia. Leaves were carefully rinsed with bi-distilled water, dried at shade and then were refluxed for 12 hours in 80% methanol. The extract was filtrated using Whatmann No. 1 filter paper and then concentrated to dryness under reduced pressure at 40.0° C using a rotatory evaporator. The required concentration was prepared by dissolving the appropriate weight in 1.0 M HCl.

2.1. Electrochemical tests

The electrochemical experiments were performed by using a potentiostat PGZ100 directed by Voltmaster software. A cell with three electrodes was connected with the thermostat. A Pt electrode and saturated calomel electrode were used as auxiliary and reference electrodes, respectively. The same material was used for both gravimetric and electrochemical experiments. Potentiodynamic polarization tests were performed at a scan rate of 1.0 mV/s. prior to all experiments, the potential was allowed to be stable at free potential during 0.5 hour. The polarization curves were attained from

–500 mV to –100 mV. So as to investigate the effects of temperature and on CFLE effectiveness, some experiments were performed at 298–328 K temperature range.

Measurements of electrochemical impedance spectroscopy (EIS) were accomplished using the instrument (PGZ100). Prior to sine wave voltage (10 mV) peak to peak, at frequencies between 10^4 Hz and 10^{-3} Hz are superimposed on the rest potential, the steady-state current at a corrosion potential was determined, Computer programs automatically controlled the measurements performed at rest potentials after 0.50 hour of contact at 298 K. The EIS diagrams are obtained as Nyquist plots. To confirm reproducibility, all test were performed three times.

2.3. Mass loss measurements

Dimensions of samples which used throughout all tests are $2.0 \times 2.0 \times 0.08$ cm. sample composition is: (0.179% C, 0.165% Si, 0.439% Mn, 0.203% Cu, 0.034% S and Fe balance. Before each test, the surfaces of all samples were abraded using emery papers of 1200, 800, 320 and 180 grades, then rinsed thoroughly with bi-distilled water, degreased and dried with acetone. Mass loss measurements were performed at 298K for 12 hours.

3. RESULTS AND DISCUSSION

3.1. Potentiodynamic polarization curves

Figure 1 shows the Tafel polarization plots at numerous of concentrations of CFLE. The kinetic factors viz. corrosion current density (I_{corr}), cathodic Tafel slopes (b_c), anodic Tafel slopes (b_a) and corrosion potential (E_{corr}) were attained from these plots and are given in Table1. Inhibition efficiency (EI%) values were determined using Eq. 1:

$$EI\% = \frac{I_{\text{corr}}^0 - I_{\text{corr}}}{I_{\text{corr}}^0} \times 100 \quad (1)$$

where I_{corr}^0 and I_{corr} are corrosion current densities of mild steel without and with CFLE, respectively.

Table 1. Electrochemical parameters of mild steel at various concentrations of CFLE in 1.0 M HCl and corresponding inhibition efficiency.

CFLE	Conc. (g/L)	$-E_{\text{corr}}$ (mV/SCE)	I_{corr} ($\mu\text{A cm}^{-2}$)	$-b_c$ (mV dec $^{-1}$)	b_a (mV dec $^{-1}$)	$IE_{I_{\text{corr}}}$ (%)
Blank	-	398	1668	177	88	----
	1.50	409	203	214	105	87.8
CFLE	1.00	423	335	192	112	79.9
	0.50	472	539	126	114	67.7
	0.25	496	607	102	99	63.6

Results in Table 1, show that, values of I_{corr} decreased gradually with the increase of CFLE concentration. It is obvious that, values of the cathodic Tafel slopes, b_c , differ slightly except at the lowest concentration indicating that mechanism of the proton discharge reaction does not change by addition of CFLE.

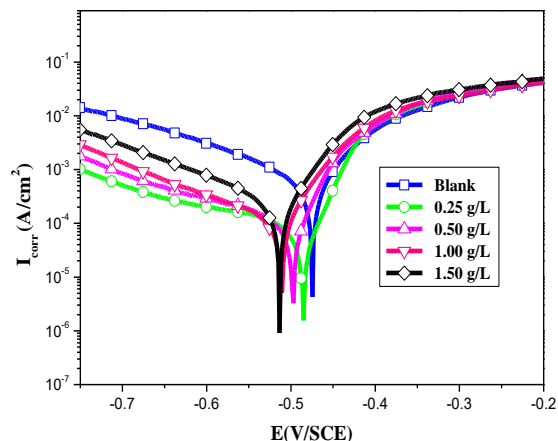


Figure 1. Potentiodynamic polarization curves of mild steel in 1.0 M HCl in the presence of different concentrations of CFLE

Figure 1 reveals that CFLE suppressed the cathodic current more than the anodic one. Inhibition efficiency (IE %) increases as the CFLE concentration increases reaching a maximum value (87.8 %) at 1.50 g/L.

3.2. Electrochemical impedance spectroscopy

Nyquist plots of mild steel in 1.0 M HCl aqueous solutions with and without CFLE are presented in Figure 2. Curves have been obtained after 0.5 hour of soaking the electrodes in the required concentration.

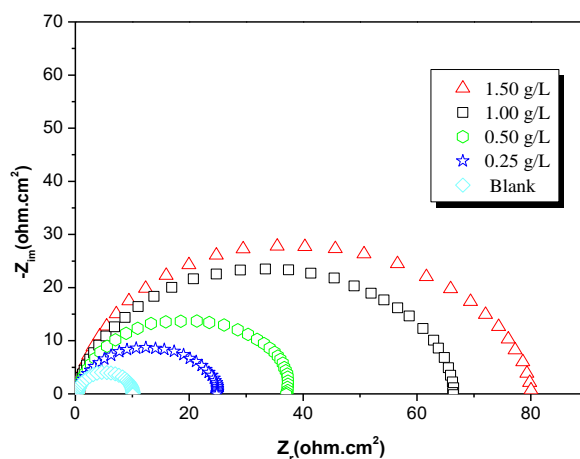


Figure 2. Nyquist diagrams for mild steel electrode with and without CFLE after 30 minutes of soaking

It is clear from Figure 2 that single capacitive loops have been obtained. The inhibition efficiencies, EI_{R_t} (%) are displayed in Table 2.

Table 2. Electrochemical Impedance parameters for corrosion of mild steel at various concentrations of CFLE

CFLE	CFLE (g/L)	R_t ($\Omega \cdot \text{cm}^2$)	f_{max} (Hz)	$(10^4) C_{dl}$ ($\mu\text{F}/\text{cm}^2$)	EI_{R_t} (%)
Blank	---	13	165	1.02	---
CFLE	0.25	36	71	32.2	63.9
	0.50	40	82	30.4	67.5
	1.00	71	65	1.06	81.7
	1.50	109	51		88.1

In order to determine R_t values, the high frequency impedance was subtracted from the low frequency one as shown in equation 2 [11]:

$$R_t = Z_{re} \text{ (at low frequency)} - Z_{re} \text{ (at high frequency)} \quad (2)$$

C_{dl} values (electrochemical double layer) were determined at the frequency f_{max} , when the imaginary component of the impedance has a maximum value ($-Z_{\text{max}}$) by equation 3 [12]:

$$C_{dl} = \frac{1}{2\pi f_{\text{max}} R_t} \quad (3)$$

The inhibition efficiency $IE\%_{(EIS)}$ is determined by using equation 4:

$$EI\%_{(EIS)} = \frac{R_t^o - R_t}{R_t^o} \times 100 \quad (4)$$

where R_t^o and R_t are the charge transfer resistance values without and with CFLE, respectively.

It is understandable from Table 2 that the resistance values increase in the presence of CFLE. This can be ascribed to the effect of corrosion protection of the molecules. It is also can be noticed that C_{dl} values decrease in the presence of CFLE. This may be ascribed to the local dielectric constant decrease and/or to the rise in the depth of the electric double layer [13- 14], indicating that CFLE molecules working by adsorption at the interface of the solution/metal. The decrease of C_{dl} values and the increase of R_t values and hence, the $IE\%$ increase is likely due to the regular substitution of water molecules by the adsorbed CFLE molecules on the steel surface, reducing the degree of Fe ionization [15-16]. The results concluded from EIS tests are in good agreement with those obtained from polarization tests.

3.3. Mass loss method

The influence of adding several concentrations of CFLE was examined by using mass loss method at 298 K. The inhibition efficiency EI_w (%) is determined by using Equation 5:

$$EI_w\% = \frac{W_{corr}^o - W_{corr}}{W_{corr}^o} \times 100 \quad (5)$$

where W_{corr}^o and W_{corr} are the corrosion rates of mild steel in 1.0 M HCl aqueous solutions

without and with of different concentrations of CFLE, respectively.

Table 3. corrosion behavior of mild steel with and without 1.0 M HCl by using mass loss method at 298K

CFLE	CFLE (g/L)	W _{corr} (mg. cm ⁻² . h ⁻¹)	EI _w (%)	Θ
Blank	---	1.124	----	
CFLE	0.25	0.458	59.3	0.593
	0.50	0.372	66.9	0.669
	1.00	0.217	80.7	0.807
	1.50	0.142	87.4	0.874

Results shown in Table 3 revealed that the inhibition effectiveness rises as the concentration of CFLE increases. It is clear that the maximum inhibition efficiency (87.4%) is found to be achieved at concentration of 1.50 g/L. These results are in agreement with that obtained by the electrochemical measurements.

3.4. Adsorption study

Adsorption study aims to discover the way by which the CFLE molecules interact with the steel surface. Values of surface coverage, θ, at various CFLE concentrations at 298K, shown in Table 3, have been employed to determine the adsorption isotherm. θ values were calculated by using Equation 6:

$$\theta = \frac{W_{corr}^0 - W_{corr}}{W_{corr}^0} \tag{6}$$

There are many models of adsorption isotherms such as, Freundlich, Temkin and Langmuir isotherms.

Application of Equation 7 gives a straight line with a slope value of 1.021. and good correlation coefficient (R² > 0.996) approving that the adsorption of the CFLE from 1.0 M HCl aqueous solutions on the mild steel surface follows the Langmuir model. Results are shown in Figure 3.

$$\frac{C_{inh}}{\theta} = \frac{1}{K_{ads}} + C_{inh} \tag{7}$$

with

$$\Delta G_{ads} = -RT \ln 55.5 K_{ads} \tag{8}$$

The equilibrium adsorption constant (K_{ads}) value was determined from the intercept of Equation 7 and ΔG_{ads} was calculated from Equation 8. The low negative value of ΔG_{ads} (-13.8 kJ/mol), suggests that adsorption of CFLE on the mild steel surface is a physical process [18-19].

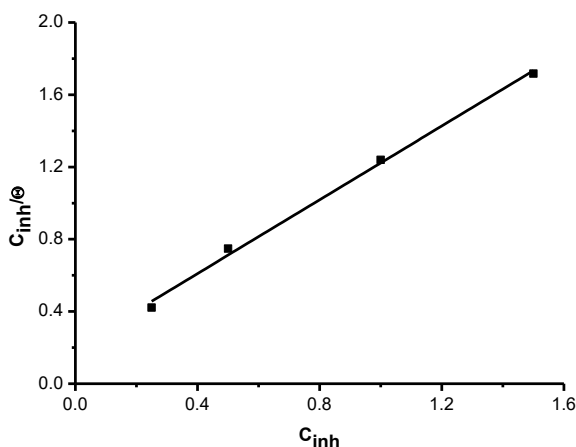


Figure 3. Langmuir isotherm plot of CFLE adsorbed on mild steel in 1.0 M HCl.

3.5. Effect of temperature

(EIS) technique was adapted to explore the effect of temperature on the inhibition process and to obtain some thermodynamic parameters of the corrosion process. EIS experiments were performed at temperature range (298-328 K) without and with the optimal concentration of CFLE (Figures 4 and 5).

Results displayed in Table 4, confirm that the charge transfer resistance decreases as the temperature increases in both inhibited and uninhibited solutions. Table 4 also revealed that IE% values in the presence of CFLE are almost constant. These results prove that CFLE is an efficient inhibitor over the studied temperature range. It is clear that CFLE efficiency is temperature independent.

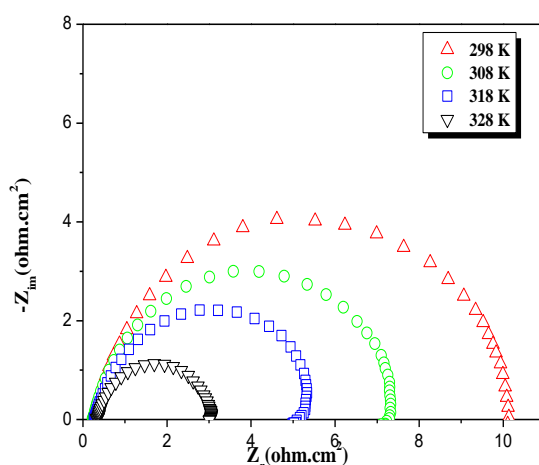


Figure 4. Nyquist diagrams for mild steel in 1.0 HCl + CFLE (1.50 g/L) at different temperatures

Equation 9 was used to calculate corrosion current density (I_{corr}) values at several temperatures in absence and existence of CFLE [22]:

$$I_{corr} = RT(zFR_t)^{-1} \quad (9)$$

where R_t is the charge transfer resistance, T is the absolute temperature, R is the gas constant ($8.31 \text{ J K}^{-1}\text{mol}^{-1}$), z is the iron valence ($z = 2$) and F is the Faraday constant

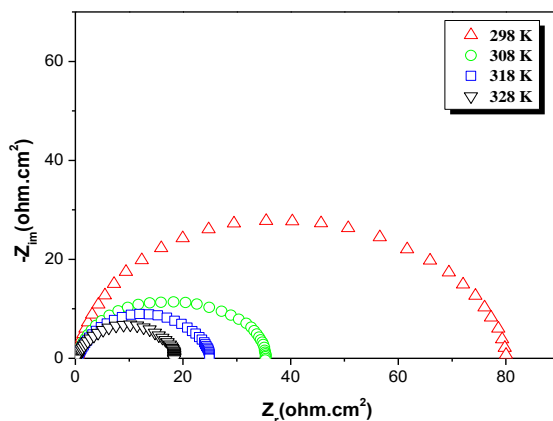


Figure 5. Nyquist diagrams for mild steel in 1.0 M HCl at different temperatures.

The activation energy (E_a) was calculated from the slope of Arrhenius equation (Equation 10) while the entropy change (ΔS) and enthalpy change (ΔH) were obtained from the intercept and slope of Eyring equation (Equation 11).

$$\ln I_{corr} = \ln A - \frac{E_a}{RT} \quad (10)$$

$$\ln \frac{I_{corr}}{T} = \frac{-\Delta H}{RT} + \ln \frac{k_B}{h} + \frac{\Delta S}{R} \quad (11)$$

where E_a is the activation energy of the corrosion process, k_B is the Boltzmann constant, T is the temperature (K), A is the Arrhenius constant, h is Planck’s constant and N is the Avogadro’s number.

Table 4. Thermodynamic parameters for the adsorption of CFLE in 1.0 M HCl on the mild steel at different temperatures.

CFLE	T (K)	R_t ($\Omega\text{.cm}^2$)	f_{max} (Hz)	C_{dl} ($\mu\text{F/cm}^2$)	EI_{Rt} (%)
Blank	298	12	161	103	---
	308	8	203	117	---
	318	6	252	130	---
	328	4	636	87	---
1.50 g/L CFLE	298	86	66	35	86.1
	308	42	82	61	81.0
	318	33	103	67	81.8
	328	22	106	91	81.6

Values of ΔS , ΔH and E_a with and without 1.5 g/L of CFLE are shown in Table 5. It is clear that the value of activation energy E_a , of the corrosion process, in the absence of the CFLE, is smaller

than that in the presence of CFLE confirming that the corrosion process becomes more difficult after adding CFLE. It is also clear that the thermodynamic parameters (ΔS and ΔH) in the existence of CFLE are lesser than those calculated in the absence of CFLE. The more positive sign of ΔH in the presence of CFLE indicates an endothermic nature of the corrosion process suggesting that the ionization of mild steel is slow [23] in the presence of inhibitor. Large and negative value of entropies (ΔS) denotes that during the rate determining step, the activated complex is formed via an association rather than a dissociation step [24], proving that a decrease in disordering takes place on going from reactants to the activated complex [25-26].

Table 5. Values of activation parameters for mild steel in 1.0 M HCl in the absence and presence of 1.50 g/L of CFLE

Inhibitor	E_a (kJ/mol)	ΔH_a (kJ/mol)	ΔS_a (J/mol)	$E_a - \Delta H_a$ (KJ/mol)
Blank	34.57	31.97	-78.35	2.6
CFLE	42.00	39.39	-69.35	2.6

3.6. Computational methods

A theoretical Calculations were performed only on the major constituent [27, 28] of *Coleus forskohlii* leaf extract which is known as forskolin (molar mass 410.51 g/mole). Figure 6 shown the chemical structure of forskolin.

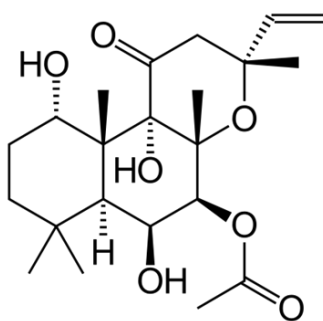


Figure 6. Molecular structure of Forskolin

Quantum chemical calculations were conducted using DMol3 program [29]. The calculations were carried out by means of Mulliken population analysis [30] and using the GGA functional method with DNP basis set and BOP functional [31]. The solvation effects (aqueous phase) were used by the COSMO [30] controls. The calculations started without any geometry constraints until full geometry optimizations. The convergence parameters were as follows: convergence energy tolerance 1×10^{-6} Ha, maximum displacement 0.005 Å, SCF tolerance 1×10^{-6} eV/atom. After the geometry optimization convergence, the following parameters were performed: The HOMO (Highest Occupied Molecular Orbital energy), LUMO (Lowest Unoccupied Molecular Orbital energy) [32] and Fukui indices (FI) [33].

3.7. DFT calculations

Global reactivity descriptors

The reactivity between corrosion inhibitors and metal surfaces depends on the molecular properties of the inhibitor such as its geometry, partial atomic charges, electronic energy, electronegativity and frontier molecular orbitals [34-35]. The presence of, particular groups on inhibitor molecules like heteroatoms, bond type, electron density and aromatic systems [36-37] can play a great role to determine the reactivity because these functional characteristic have high aptness to act as corrosion inhibitors [36]. DFT calculation usually used to explain the mechanism of corrosion inhibition in terms of electronic and molecular structure properties. The optimized molecular structure of Forskolin obtained from the calculations is shown in Figure 7a. The HOMO and LUMO orbitals are shown in Figures 7b and 7c. The HOMO orbitals is considered as the active centers of the molecule which characterized by the highest tendency to bond to the surface of the metal, thus it is the position where the electrophiles attack occur. However, the LUMO orbital can receive electrons from the d-orbital of the metal (Fe) and makes antibonding orbitals to form feedback bonds [37].

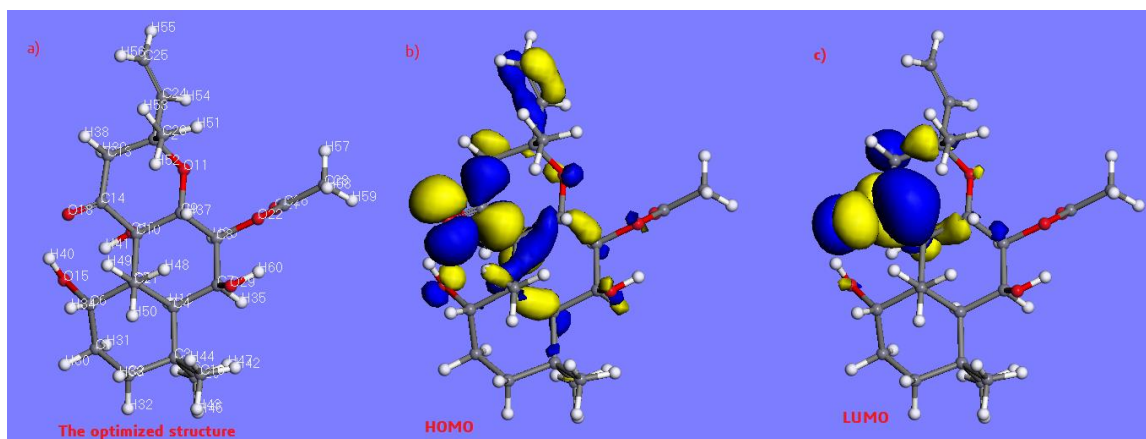


Figure 7. (a) Optimized molecular structure, (b) frontiers orbitals distribution HOMO and (c) LUMO of Forskolin

The ionization potential (IP), electron affinity (EA) are related to E_{HOMO} and E_{LUMO} using the Equations (12) and (13) [38]:

$$IP = -E_{HOMO} \quad (12)$$

$$EA = -E_{LUMO} \quad (13)$$

Mulliken electronegativity (χ) and Absolute hardness (η) can be determined by using Equations (14) and (15) [39-40]:

$$\chi = \frac{IP + EA}{2}, \quad \chi = -\frac{E_{LUMO} + E_{HOMO}}{2} \quad (14)$$

$$\eta = \frac{IP - EA}{2}, \quad \eta = -\frac{E_{LUMO} - E_{HOMO}}{2} \quad (15)$$

The number of transferred electrons ΔN can be deduced by application of the Pearson method using equation (16) [41]:

$$\Delta N = \frac{\chi_{Fe} - \chi_{inh}}{2(\eta_{Fe} - \eta_{inh})} \quad (16)$$

Where χ_{Fe} and χ_{inh} are the absolute electronegativity of Iron and inhibitor molecule respectively, η_{Fe} and η_{inh} are the absolute hardness of Iron and the inhibitor molecule respectively. A theoretical values of $\chi_{Fe} = 7\text{eV}$ and $\eta_{Fe} = 0$ (since for bulkmetallic atoms $I = A$) were used to calculate the ΔN value [42,43]. Recently, it was demonstrated that the value of $\chi_{Fe} = 7\text{ eV}$ is theoretically not acceptable since electron-electron interactions were not considered, only free electron gas Fermi energy of iron was considered [44–46]. The work function (ϕ) of the metal surface is usually used by researchers, instead of χ_{Fe} , as it is more suitable measure for electronegativity [44–46]. The obtained value of the (ϕ) function for Fe (1 1 0) surface is 4.82 eV [44,45]. The equation (16) is rewritten as follows:

$$\Delta N = \frac{\phi - \chi_{inh}}{2(\eta_{Fe} + \eta_{inh})} \quad (17)$$

The quantum chemical parameters of Forskolin determined from the DFT calculation (E_{HOMO} , E_{LUMO} , ΔE_{gap} , ΔN_{110}) are summarized in Table 6.

Table 6. The quantum chemical parameters of Forskolin from the DFT calculation

Inhibitor	E_{HOMO} (eV)	E_{LUMO} (eV)	ΔE_{gap} (eV)	ΔN_{110}
Forskolin	-5.438	-2.064	3.373	0.31

The ability of Forskolin molecule to give electron to an acceptor (Iron) is measured by the HOMO energy (E_{HOMO}), while the proclivity of Forskolin molecule to receive electron from Iron is measured by the LUMO energy (E_{LUMO}) [51]. High values of E_{HOMO} (-5.438 eV) show a trend of Forskolin molecule to give electrons to Iron with low energy or an empty electron orbital, i.e. vacancies in the 3d orbital of the Iron atom. The E_{LUMO} characterizes the susceptibility of molecules towards nucleophilic attack [31-36]. Low values of the gap $\Delta E = E_{LUMO} - E_{HOMO}$ (3.373 eV) indicate that the energy required to remove an electron from the last occupied orbital will be reduced, corresponding to improved inhibition efficiencies. Therefore, higher E_{HOMO} and/or lower E_{LUMO} favor(s) higher corrosion inhibition strength [51]. On the other hand, ΔN_{110} value (0.31), indicates the ability of tested inhibitor to transfer its electrons to metal, if $\Delta N > 0$ and vice versa if $\Delta N < 0$ [53,54]. According to above interpretation, the forskohlin molecule has higher tendency to donate electrons to Iron surface.

Fukui Indices

The Fukui Function (FI) are important tools for predicting the regioselectivity of the forskolin molecule and its reactive regions in terms of nucleophilic (f^+) and electrophilic attack (f^-) [55]. The condensed Fukui function in terms of the atomic charges are given by:

$$f_k^- = q_k(N) - q_k(N - 1) \text{ (for electrophilic attack)}$$

$$f_k^+ = q_k(N + 1) - q_k(N) \text{ (for nucleophilic attack)}$$

Where q_k is the electronic charge of atom k and N is the number of electrons.

Results show that the preferred site for nucleophilic attack (shown by the highest value of f^+) is on C (14) while the highest values of f^- are on O (18). The results obtained from Fukui function and from the analysis of the LUMO and HOMO orbitals are in good agreement, the two methods lead to the same predictions of the site with most electron deficient. The results obtained for these regions in electrophilic and nucleophilic attacks support the high capability of tested compound to react with surface of metal through donor-acceptor interactions between most reactive sites of the inhibitor molecule (forskohlin) and Iron surface.

3.8 Scanning electron microscopy

To support our conclusion that CFLE diminishes the corrosion degree by means of formation of a protecting layer on the steel surface, the SEM analysis was performed in absence and presence of 1.5g/L of CFLE. Figure 8(a) reveals that the surface of the mild steel is highly damaged due to rapid corrosion attack in acidic solution. However, there is a clear difference in the surface morphology of the mild steel in presence of inhibitor. In fact, there is a fewer pits and cracks Figure 8(b), showing that the inhibitor molecules have been adsorbed on the steel surface and the corrosion process is suppressed [56].

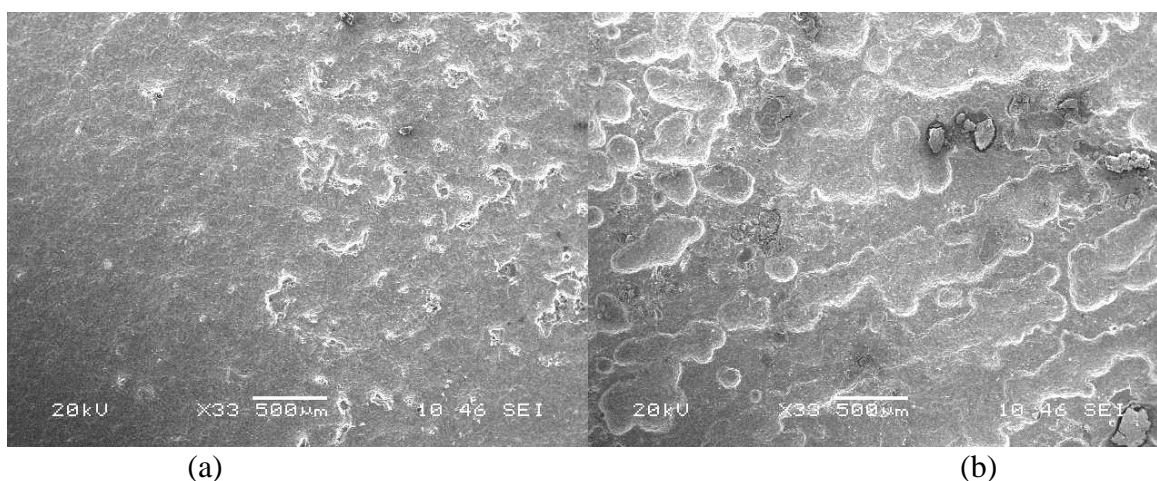


Figure 8. SEM images of MS: (a) in 1.0 M HCl and (b) in 1.0 M HCl + 1.50 g/L of CFLE after 12 h of immersion time at 298 K

3.9 (EDS) test

The EDS spectra were utilized to measure the elements found on the surface of mild steel after 24hrs of soaking in the lack and presence of CFLE. Results are shown in Figure 9. It is clear that the Fe ratio in the presence of CFLE is higher than that in the absence of CFLE, indicating more Fe dissolves (ionizes) in the absence of CFLE, this confirms the efficiency of the studied inhibitor.

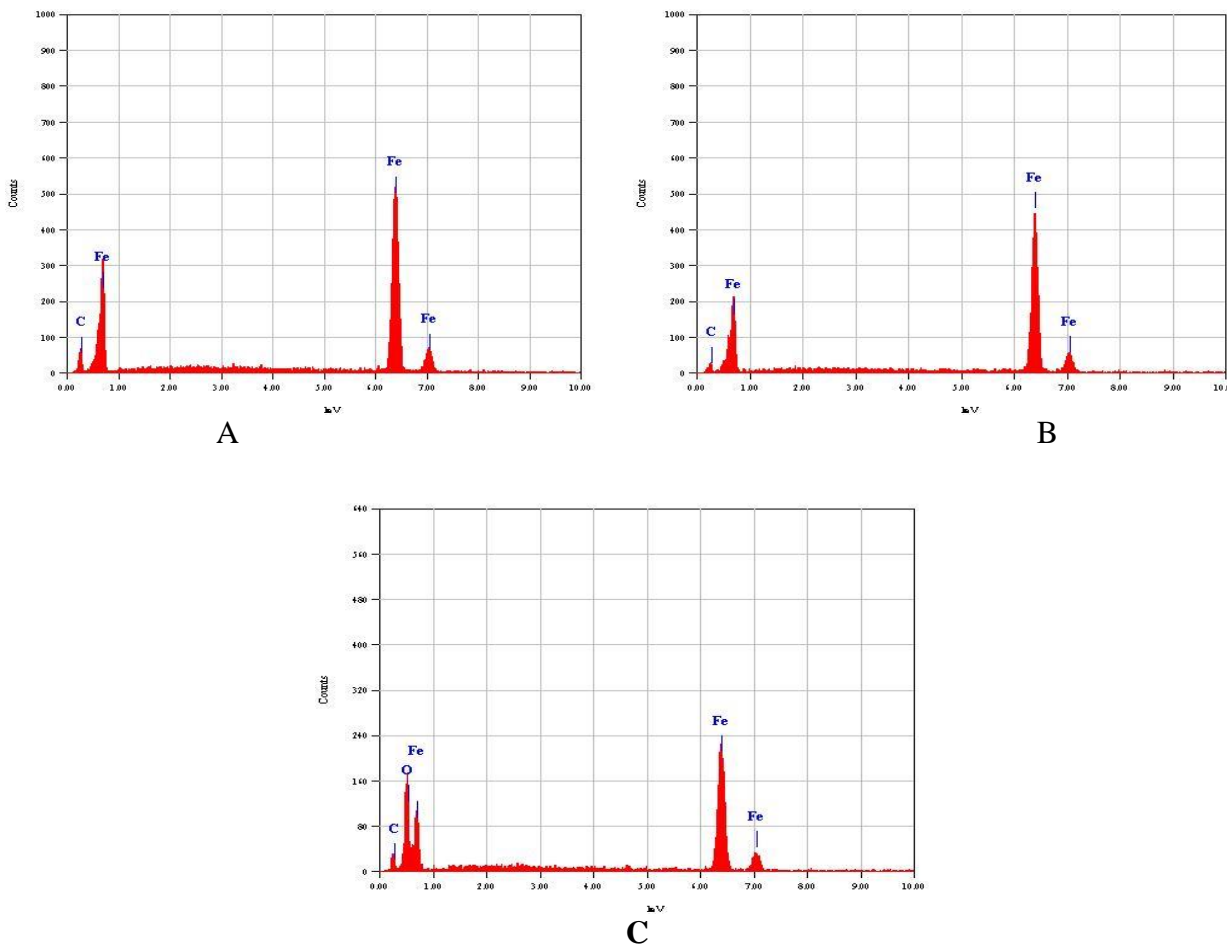


Figure 9. EDS study of mild steel after immersion for 24hrs (a) without corrosion medium and CFLE (b) in the presence of 1.50 g/L of CFLE in 1.0 M HCl solution (c) in 1.0 HCl solution and without CFLE

3. 10 Comparison of CFLE with other natural corrosion inhibitors

Comparison the maximum inhibition efficiency (IE%) of CFLE with those of various natural inhibitors stated in the literature is given in Table 7. The variation of IE% could ascribed to the differences in the constituent of each plant. Table 7 revealed that CFLE can be classified as one of the most efficient corrosion green inhibitors.

Table 7. Comparison of maximum corrosion inhibition efficiency (IE) of various plant extracts for mild steel

Inhibitor	Maximum IE%	Reference
Leaves of <i>Coleus forskohlii</i>	88.1	This study
Roots of <i>Rotula aquatica</i>	86.6	4
Leaves of <i>Jathropha curcas</i>	85.6	57
Fenugreek gum	94.0	58
Flowers of <i>Cassia auriculata</i>	74.4	59
Leaves of <i>Vitex doniana</i>	68.7	60

4. CONCLUSIONS

From the above discussion, it has been proved that, CFLE is an excellent corrosion inhibitor for the mild steel over the temperature range of (298 – 328K) in 1.0 M HCl aqueous solutions. The inhibition efficiency of CFLE increases as the concentration increases. The efficiency is also enhanced slightly with increasing temperature. CFLE acts as a mixed-type corrosion inhibitor, hindering both the cathodic and anodic processes of the corrosion reaction. The adsorption of CFLE on the mild steel surface was found to obey the Langmuir model. The ΔG_{ads} value shows that the adsorption process has a spontaneous nature. It is also concluded from the DFT calculations that CFLE has higher tendency to be adsorbed on the metal surface.

ACKNOWLEDGEMENT

The authors extend their appreciation to the Deanship of Scientific Research at King Khalid University for funding this work through research groups program under grant number R.G.P.1/25/38.

References

1. H. K. Gerhardus, P. H. Michiel, Y. P. Virmani and J. H. Payer, *Corrosion Costs and Preventive Strategies in the United States*, 1 (2002) 1562.
2. L. Herrag, B. Hammouti, S. Elkadiri, A. Aouniti, C. Jama, H. Vezin and F. Bentiss, *Corros. Sci.*, 52 (2010) 3042.
3. S. R. Al-Mhyawi, *Afr. J. Pure Appl. Chem.*, 8 (2014) 9.
4. N. S. Patel, J. Hadlicka, P. Beranek, R. Salghi, H. Bouya, H. A. Ismat and B. Hammouti, *Port. Electrochim. Acta*, 32 (2014) 395.
5. O. I. El Mouden, A. Anejjar, M. Messali, R. Salghi, H. A. Ismat and B. Hammouti, *Chem. Sci. Rev. Lett.*, 3 (2014) 579.
6. I. H. Ali and M. I. Khan, *Int. J. Electrochem. Sci.*, 12 (2017) 2285.
7. A. Chaouiki, H. Lgaz, I. Chung, I. H. Ali, S. L. Gaonkar, K. S. Bhat, R. Salghi, H. Oudda and M. I. Khan, *J. Mol. Liq.*, 266 (2018) 603.
8. M. S. Al-Otaibi, A. M. Al-Mayouf, M. Khan, A. A. Mousa, S. A. Al-Mazroa and H. Z. Alkhatlan, *Arab. J. Chem.*, 7 (2014) 340.
9. H. Lgaz, K. S. Bhat, R. Salghi, Shubhalaxmi, S. Jodeh, M. Algarra, B. Hammouti, I. H. Ali and A. Essamri, *J. Mol. Liq.*, 238 (2017) 71.
10. R. Salghi, S. Jodeh, E. E. Ebenso, H. Lgaz, B. D. Hmamou, I. H. Ali, M. Messali, B. Hammouti and N. Benchat, *Int. J. Electrochem. Sci.*, 12 (2017) 3309.
11. A. A. Al-Amierya, M. H. O. Ahmed, T. A. Abdullah, T. S. Gaaz, A. A. H. Kadhum, *Results in Physics*, 9 (2018) 978.
12. E. Ituen, A. James, O. Akaranta and S. Sun, *J. Chem. Eng.*, 24 (2016) 1442.
13. S. A. Umoren, *Journal of Adhesion Science and Technology*, 30 (2016) 1858.
14. D. I. Njoku, I. Ukaga, O. B. Ikenna, E. E. Oguzie, K. L. Oguzie and N. J. Ibis, *J. Mol. Liq.*, 219 (2016) 417.
15. K. K. Alaneme, S. J. Olusegun and A. W. Alo, *Alexandria Engineering Journal*, 55 (2016) 1069.
16. S. Kumar, *Protection of Metals and Physical Chemistry of Surfaces*, 52 (2016) 376.
17. M. Jokar, T. S. Farahani and B. Ramezanzadeh, *Journal of the Taiwan Institute of Chemical Engineers*, 63 (2016) 436.

18. R. Venegas, F. Figueredo, G. Carvallo, A. Molinari and R. Vera, *Int. J. Electrochem. Sci.*, 11(2016) 3651.
19. A. A. Khadoma, A. N. Abdb and N. A. Ahmed, *South African Journal of Chemical Engineering*, 25 (2018) 13.
20. B. Raja and M. G. Sethuraman, *Materials Letters*, 62 (2008) 113.
21. I. H. Ali and M. H. A. Suleiman, *Int. J. Electrochem. Sci.*, 13 (2018) 3910.
22. R. Salghi, S. Jodeh, E. E. Ebenso, H. Lgaz, D. B. Hmamou, M. Belkhaouda, I. H. Ali, M. Messali, B. Hammouti and S. Fattouch, *Int. J. Electrochem. Sci.*, 12 (2017) 3283.
23. I. H. Ali and Y. Sulfab, *Transition Met. Chem.*, 38 (2013) 79.
24. V. R. Saliyan and A. V. Adhikari, *Bull. Mater. Sci.*, 31 (2008) 699.
25. I. H. Ali, *Russian Journal of Physical Chemistry A*, 89 (2015) 987.
26. F. Bentiss, M. Lebrini and M. Lagrenee, *Corros. Sci.*, 47 (2005) 2915.
27. C. Kavitha, K. Rajamani and E. Valivel, *J. Med. Plant. Res.*, 4 (2010) 278.
28. N. J. De Souza and V. Shah, *Econ. Med. Plant Res.*, 2 (1988) 1.
29. B. Delley, *J. Chem. Phys.*, 113 (2000) 7756.
30. R. S. Mulliken, *J. Chem. Phys.*, 23 (1955) 1833.
31. B. Delley, *J. Phys. Chem. A*, 110 (2006) 13632.
32. M. J. Dewar and M. Thiel, *J. Am. Chem. Soc.*, 99 (1977) 4899.
33. R. N. Singh, A. Kumar, R. K. Tiwari and P. Rawat, *Spectrochim. Acta. A. Mol. Biomol. Spectrosc.*, 112 (2013) 182.
34. H. Jafari, I. Danaee, H. Eskandari and M. RashvandAvei, *J. Mater. Sci. Technol.*, 30 (2014) 239.
35. L. M. Rodríguez-Valdez, M. Villamizar, M. Casales, J. G. González-Rodríguez, A. MartínezVillafañe, L. Martinez and D. Glossman-Mitnik, D., *Corros. Sci.*, 48 (2006) 4053.
36. D. Daoud, T. Douadi, H. Hamani, S. Chafaa and M. Al-Noaimi, *Corros. Sci.*, 94 (2015) 21.
37. F. E. Awe, S. O. Idris, M. Abdulwahab and E.E. Oguzie, *Cogent Chem.*, 1 (2015) 1112676.
38. M. Gholami, I. Danaee, M. H. Maddahy and M. RashvandAvei, *Ind. Eng. Chem. Res.*, 52 (2013) 14875.
39. R. G. Pearson, *Inorg. Chem.*, 27 (1988) 734.
40. V. Sastri and J. Perumareddi, *Corrosion*, 53 (1997) 617.
41. S. Martinez, *Mater. Chem. Phys.*, 77 (2003) 97.
42. A. Y. Musa, A. A. H. Kadhum, A. B. Mohamad, M. S. Takriff, *Mater. Chem. Phys.*, 129 (2011) 660.
43. H. Shokry, *J. Mol. Struct.*, 199 (2014) 80.
44. Z. Cao, Y. Tang, H. Cang, J. Xu, G. Lu and W. Jing, *Corros. Sci.*, 83 (2014) 292.
45. A. Kokalj, *Chem. Phys.*, 393 (2012) 1.
46. I. Obot, D. Macdonald and Z. Gasem, *Corros. Sci.*, 99 (2015) 1.
47. H. Lgaz, R. Salghi, M. Larouj, M. Elfaydy, S. Jodeh, Z. Rouifi, B. Lakhrissi and H. Oudda, *J. Mater. Environ. Sci.*, 7 (2016) 4471.
48. A. O. Yüce, E. Telli, B. D. Mert, G. Kardaş and B. Yazıcı, *J. Mol. Liq.*, 218 (2016) 384.
49. A. Liu, X. Ren, J. Zhang, C. Wang, P. Yang, J. Zhang, M. An, D. Higgins, Q. Li and G. Wu, *RSC Adv.*, 4 (2014) 40606.
50. Y. El Aoufir, H. Lgaz, H. Bourazmi, Y. Kerroum, Y. Ramli, A. Guenbour, R. Salghi, F. El-Hajjaji, B. Hammouti and H. Oudda, *J. Mater. Environ. Sci.*, 7 (2016) 4330.
51. M. Messali, H. Lgaz, R. Dassanayake, R. Salghi, S. Jodeh, N. Abidi and O. Hamed, *J. Mol. Struct.*, 1145 (2017) 43.
52. N. A. Wazzan, *J. Ind. Eng. Chem.*, 26 (2015) 291.
53. A. Kokalj, *Electrochimica Acta*, 56 (2010) 745.
54. N. Kovačević and A. Kokalj, *Corros. Sci.*, 53 (2011) 909.
55. H. Lgaz, R. Salghi and I. H. Ali, *Int. J. Electrochem. Sci.*, 13 (2018) 250.
56. I. H. Ali, *Int. J. Electrochem. Sci.*, 11 (2016) 2130.

57. J. K. Odusote and O. M. Ajayi, *Journal of Electrochemical Science and Technology*, 4 (2013) 81.
58. H. Lgaz, I. Chung, R. Salghi, I. H. Ali, A. Chaouiki, Y. El Aoufir and M. I. Khan, *Applied Surface Science*, 463 (2019) 647.
59. J. R. Vimala, A. L. Rose and S. Raja, *Int.J. Chem. Tech. Res.*, 3 (2011) 1791.
60. O. T. Uzoma, I. I. Maryjane, U. E. Thompson, A. V. I., Egbulefu and U. N. Lilian, *J. Chem. Chem. Eng.*, 6 (2012) 708.

© 2018 The Authors. Published by ESG (www.electrochemsci.org). This article is an open access article distributed under the terms and conditions of the Creative Commons Attribution license (<http://creativecommons.org/licenses/by/4.0/>).